Pergamon

*Int. J. Solids Structures* Vol. 35, No. 16, pp. 1895–1913, 1998

0020–7683/98 $19.00 + .00

PII: S0020–7683(97)00128–5

# HOMOGENIZED NONLINEAR CONSTITUTIVE LAW USING FOURIER SERIES EXPANSION

ERICK PRUCHNICKI
Laboratoire de Mécanique de Lille, CNRS URA 1441 Ecole Centrale de Lille, Cité Scientifique, B.P. 48, 59651 Villeneuve d'Ascq cédex, France

(*Received* 14 *September* 1996; *in revised form* 30 *April* 1997)

**Abstract**—This work is concerned with modeling the nonlinear homogenized elastoplastic behavior of a composite comprised of a periodic microstructure under small deformation conditions. A Fourier series approach is used in solving the integral equation [called the periodic Lippmann–Schwinger's equation, Kröner, E. (1972) *Statistical Continuum Mechanics*, p. 110. Springer, Wien] which governs the micromechanical behavior of the composite material. The nonlinear behavior of fibrous composite is approximated by discretizing the unit cell into subregions in which microplastic strain tensor is assumed to be constant. The method is applied to the case where the individual constituents are elastic-perfectly plastic Von-Mises materials. The elastoplastic homogenized law is used to analyze the behavior of a fibrous boron/aluminum metal–matrix composite under various loading paths. © 1998 Elsevier Science Ltd.

## 1. INTRODUCTION

The last three decades have seen important developments of heterogeneous materials in science and technology. These materials have the interesting mechanical properties of stiffness, lightness and strength, which are impossible to obtain with homogeneous materials. However, analysis of these structures implies some difficulties. Because of the complexity of pieces and the order of size of heterogeneity, it is very expensive to compute a structure directly. The discretization must be thinner than the size of heterogeneity. Therefore, the homogenization method is very interesting.

The homogenization process consists of replacing the heterogeneous composite structure by homogeneous medium with anisotropic properties, which have to be determined. The homogenization theory of periodic media deals with the limit behavior of composite materials when their structure becomes thinner and thinner (Sanchez-Palencia, 1980; Bensoussan *et al.*, 1978). This law, called homogenized behavior, relates the macrostress ($\mathbf{\Sigma}$) and macrostrain ($\mathbf{E}$) tensors, which are average over the representative volume element (r.v.e.) of the heterogeneous material of the corresponding microquantities. In the case of periodic media, the representative elementary volume, which generates by periodicity the entire structure of the composite, is called the unit cell. Aboudi (1986, 1991) models the unit cell by an assembly of parallelopiped blocks. This work expands the heterogeneous displacement throughout each part of the unit cell as linear and higher-order functions of the coordinates. The microstress and microstrain can also be numerically computed by the finite element method (Devries *et al.*, 1989; Ghosh *et al.*, 1995; Guedes, 1990; Guedes and Kikuchi, 1991; Lene, 1987; Jansson, 1992; Toledano and Murakami, 1987). A more general approach is adopted in the present work, where the displacement strain and stress fields are not restricted to linear or quadratic variations throughout some parts of the unit cell, but vary according to the assumption of periodicity, which implies that heterogeneous microfields can be expanded in an infinite Fourier series. It has been established that both the Fourier series method and the Green's function formulation are equivalent (Walker *et al.*, 1990). The theory has been introduced in elasticity by Nemat-Nasser and Taya (1981), and Nemat-Nasser *et al.* (1982). A simplified expression of homogenized elastic tensor can be obtained with assumption of constant approximation of the transformation strain tensor within each subregion dividing the unit cell (Iwakuma and Nemat-Nasser, 1983; Nemat-Nasser and Taya, 1985; Nemat-Nasser *et al.*, 1986, 1993; Suquet, 1990). This assumption has also allowed us to find bounds on the overall elastic and instantaneous elastoplastic moduli of homogenized material (Accorsi and Nemat-Nasser, 1986). Walker *et al.* (1991, 1993) have extended this approach to elastoviscoplasticity with thermal effect. Avoiding any assumption on microstrain field, Dumontet (1983) has also given a theory to define the elastic homogenized coefficient. The purpose of the present paper is to extend this development to the case where the constituents exhibit elastoplastic behavior.

In the case of multilayered media, it has been established that both the microstress and microstrain tensors are constant in each constituent. This result permits the thermodynamical formulation of an explicit macroconstitutive law for elastoplastic multilayered media (Pruchnicki and Shahrour, 1992, 1994).

In the general case of geometry (for example, fiber-reinforced material), the macroconstitutive nonlinear elastoplastic law requires, theoretically, an infinite number of internal variables which constitute the whole field of microplastic strain over the unit cell (Suquet, 1987). Once the complexity of the homogenized law is recognized, we turn to approximate models in order to obtain more quantitative results. These approximate models are based on an *a priori* feeling of the distribution of microplastic strains. Microplastic strain is assumed constant in each part where the unit cell has been partitioned (Suquet, 1983; Pruchnicki and Shahrour, 1993; Pruchnicki, 1996). This simplified theory of the hardening homogenized flow rule will be illustrated by a numerical study with a metal–matrix composite.

## 2. THEORETICAL DEVELOPMENTS

### 2.1. *Formulation of the basic problem*

Consider a periodic inhomogeneous body, comprising of two isotropic constituents (Fig. 1). Fiber inclusion is denoted by index 1 and matrix is defined by index 2 (Fig. 1). An associated elastoperfectly-plastic standard generalized II (Halphen and Nguyen, 1975) behavior is assumed for both constituents. Perfect bonding is also assumed between the two constituents. The body has two length scales, a global length scale ($x$) that is proportional to the size of the body, and a local length scale ($y$) that is of the order of the microstructure (Fig. 1). The unit cell $Y$ is a period characteristic of the material which has been enlarged by the homothetics of scaling ($1/\varepsilon = y/x$) between the two length scales (Fig. 1). The determination of the homogenized elastoplastic law requires solving the following problem over the unit cell which satisfies by microstress ($\sigma$) and microstrain ($e$) tensors.

$$\mathrm{div}_y(\boldsymbol{\sigma}(y)) = 0 \quad \text{in } Y \tag{1}$$

$$\boldsymbol{\sigma}(y) = \mathbf{a}(y):(\mathbf{e}(u(y)) - \mathbf{e}^{\mathrm{p}}(y)) \quad \text{in } Y \tag{2}$$

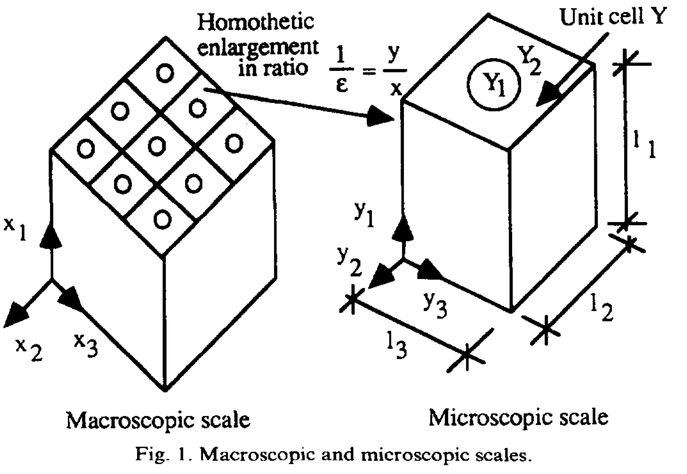


Fig. 1. Macroscopic and microscopic scales.

$$\forall \boldsymbol{\sigma}(y) \in DE \, \forall \bar{\boldsymbol{\sigma}}(y) \in DE (\boldsymbol{\sigma}(y) - \bar{\boldsymbol{\sigma}}(y)) : \dot{\mathbf{e}}^{\mathrm{p}} \geqslant 0$$

$$\mathbf{e}(u), \mathbf{e}^{\mathrm{p}}(y) \quad \text{and} \quad \boldsymbol{\sigma}(y) \text{ are } Y\text{-periodic in } y, \tag{3}$$

where $DE$ and $\mathbf{e}^{\mathrm{p}}(y)$ denote, respectively, the yield convex surface and the microplastic strain tensor.

When the stiffness tensor $(\mathbf{a}(y))$ is constant in each constituent, we have:

$$\mathbf{a}_{ijkh}(y) = (a_\alpha)_{ijkh} = \lambda_\alpha \delta_{ij} \delta_{kh} + \mu_\alpha (\delta_{ik} \delta_{jh} + \delta_{ih} \delta_{jk}) \quad \forall y \in Y_\alpha \quad (\alpha = 1, 2)$$

where $\lambda_\alpha$ and $\mu_\alpha$ denote the Lamé constants of the $\alpha$th constituent and $\delta$ denotes the Kronecker's symbol. The assumption of $Y$ periodicity of microstrain $\mathbf{e}(u)$ implies that the displacement field $u$ splits into a linear part $\mathbf{E} \cdot y$ and a periodic part $\mathbf{v}(y)$ (Lene, 1987):

$$u(y) = \mathbf{E} \cdot y + \mathbf{v}(y). \tag{4}$$

2.2. *Solution to local problem using Fourier series expansion*

We propose to solve the problem by means of a Fourier series development of the periodic microstress, microstrain and transformation strain tensor $\tilde{\mathbf{e}}(y)$, introduced for the first time by Nemat-Nasser and Taya (1981):

$$\tilde{\mathbf{e}}(y) = AP^{-1} : (\mathbf{E} + \mathbf{e}(\mathbf{v}(y)) - \mathbf{e}^{\mathrm{p}}(y)) \quad \forall y \in Y_1 \tag{5}$$

$$\tilde{\mathbf{e}}(y) = 0 \quad \forall y \in Y_2 \quad \text{with } AP = (a_2 - a_1)^{-1} : a_2. \tag{6}$$

In taking into account eqns (4)–(6), which define the transformation strain tensor, the formula (2) becomes:

$$\boldsymbol{\sigma}(y) = a_2 : (E + \mathbf{e}(\mathbf{v}(y)) - \mathbf{e}^{\mathrm{p}}(y) - \tilde{\mathbf{e}}(y)) \quad \text{in } Y \tag{7}$$

$$\mathbf{e}(v(y)) = \tfrac{1}{2}(\mathrm{grad}_y(\mathbf{v}(y)) + \mathrm{grad}_y(\mathbf{v}(y))^{\mathrm{T}}) \quad \text{in } Y$$

$$\mathbf{v}(y), \tilde{\mathbf{e}}(y) \quad \text{and} \quad \boldsymbol{\sigma}(y) \text{ are } Y\text{-periodic in } y. \tag{8}$$

Because of the periodicity with respect to the microscopic scale, the displacement, stress, and strain fields can be expressed in the Fourier series as:

$$\mathbf{v}(y) = \sum_{n=-\infty}^{+\infty} \mathbf{v}^*(n) \, \mathrm{e}^{2\pi i N \cdot y} \quad \text{in } Y \tag{9}$$

$$\mathbf{e}(\mathbf{v}(y)) = \sum_{n=-\infty}^{+\infty} \mathbf{e}^*(n) \, \mathrm{e}^{2\pi i N \cdot y} \quad \text{in } Y \tag{10}$$

$$\tilde{\mathbf{e}}(y) = \sum_{n=-\infty}^{+\infty} \tilde{\mathbf{e}}^*(n) \, \mathrm{e}^{2\pi i N \cdot y} \quad \text{in } Y \tag{11}$$

$$\mathbf{e}^{\mathrm{p}}(y) = \sum_{n=-\infty}^{+\infty} \mathbf{e}^{\mathrm{p}*}(n) \, \mathrm{e}^{2\pi i N \cdot y} \quad \text{in } Y \tag{12}$$

here $i$ is not an index and is used to indicate $\sqrt{-1}$, $n$ denotes a triplet of integers $(n_1, n_2, n_3)$, and the symbol $\sum_{n=-\infty}^{+\infty}$ represents the following triple sum:

$$\sum_{n=-\infty}^{+\infty} = \sum_{n_1=-\infty}^{+\infty} \sum_{n_2=-\infty}^{+\infty} \sum_{n_3=-\infty}^{+\infty} .$$

$N$ represents $(N_1, N_2, N_3) = (n_1/l_1, n_2/l_2, n_3/l_3)$; where $l_i$ $(i = 1\text{–}3)$ denotes the dimensions of the parallelopiped unit cell in the $y_1$, $y_2$, $y_3$ directions (Fig. 1). The notation $N \cdot y$ represents $N_1 y_1 + N_2 y_2 + N_3 y_3$.

The Fourier coefficient is given by the inverses formulation:

$$\mathbf{v}^*(n) = \frac{1}{|Y|}\int_Y \mathbf{v}(y)\, e^{-2\pi i N\cdot y}\, dY$$

$$\mathbf{e}^*(n) = \frac{1}{|Y|}\int_Y \mathbf{e}(\mathbf{v}(y))\, e^{-2\pi i N\cdot y}\, dY$$

$$\tilde{\mathbf{e}}^*(n) = \frac{1}{|Y|}\int_Y \tilde{\mathbf{e}}(y)\, e^{-2\pi i N\cdot y}\, dY \tag{13}$$

$$\mathbf{e}^{p*}(n) = \frac{1}{|Y|}\int_Y \mathbf{e}^{p}(y)\, e^{-2\pi i N\cdot y}\, dY \tag{14}$$

where $|Y|$ denotes the volume of the unit cell.

Using formulas (1) and (7)–(12), we are also in a position to establish that (see Appendix A):

$$\mathbf{e}^*(0) = 0 \tag{15a}$$

$$\mathbf{e}^*(n) = \mathbf{K}(n):(\tilde{\mathbf{e}}^*(n) + \mathbf{e}^{p*}(n)) \quad \text{for } n^2 = n_1^2 + n_2^2 + n_3^2 \neq 0, \tag{15b}$$

$\mathbf{K}(n)$ is a fourth-order tensor defined in Appendix A.

The formula (5) may be written as:

$$AP:\tilde{\mathbf{e}}(y) - \mathbf{e}(\mathbf{v}(y)) = \mathbf{E} - \mathbf{e}^{p}(y) \quad \forall y \in Y_1. \tag{16}$$

In taking into account formulas (10), (15a), (15b) and (16), we arrive at periodic Lippmann–Schwinger's equation (Kröner, 1972):

$$AP:\tilde{\mathbf{e}}(y) - \sum_{n=-\infty}^{+\infty}{}' \mathbf{K}(n):(\tilde{\mathbf{e}}^*(n) + \mathbf{e}^{p*}(n))\, e^{2\pi i N\cdot y} = \mathbf{E} - \mathbf{e}^{p}(y) \quad \forall y \in Y_1. \tag{17}$$

The prime on the triple summation signs indicates that the term with $n_1 = n_2 = n_3 = 0$ is excluded from the sum.

By multiplying each side of relation (17) by $e^{-2i\pi Q y}$ and integrating over the volume of the inclusion, we obtain the system which satisfies the Fourier expansion coefficients of the transformation strain tensor $\tilde{\mathbf{e}}(y)$ defined previously by formula (13):

$$AP:\tilde{\mathbf{e}}^*(q)\,|Y| - \sum_{n=-\infty}^{+\infty}{}' \mathbf{K}(n):\tilde{\mathbf{e}}^*(n)\mathbf{I}(q-n) = \mathbf{F}(q) \quad \forall q \tag{18}$$

$q$ denotes the triplet $(q_1, q_2, q_3)$, $q_i$ (for $i = 1\text{–}3$) are integers.

$\mathbf{F}(q)$ is defined by:

$$\mathbf{F}(q) = \mathbf{E}\mathbf{I}(q) - \mathbf{I}_1^{\mathrm{p}}(q) + \sum_{n=-\infty}^{+\infty}{}' \mathbf{K}(n) : \mathbf{e}^{\mathrm{p}*}(n)\mathbf{I}(q-n).$$

The integrals introduced in previous relations are defined as:

$$\mathbf{I}(q) = \int_{Y_1} \mathrm{e}^{-2\pi i Q\cdot y}\,\mathrm{d}y, \quad \mathbf{I}_1^{\mathrm{p}}(q) = \int_{Y_1} \mathbf{e}^{\mathrm{p}}(y)\,\mathrm{e}^{-2\pi i Q\cdot y}\,\mathrm{d}y.$$

$Q$ represents $(Q_1, Q_2, Q_3) = (q_1/l_1, q_2/l_2, q_3/l_3)$.

The real and the imaginary components of the relation (18) can be separated as follows:

$$AP : \tilde{\mathbf{a}}^*(q)\,|Y| - \sum_{n=-\infty}^{+\infty}{}' \mathbf{K}(n) : (\tilde{\mathbf{a}}^*(n)\mathbf{I}_c(q-n) + \tilde{\mathbf{b}}^*(n)\mathbf{I}_s(q-n)) = \mathbf{F}_a(q)$$

$$-AP : \tilde{\mathbf{b}}^*(q)|Y| - \sum_{n=-\infty}^{+\infty}{}' \mathbf{K}(n) : (\tilde{\mathbf{a}}^*(n)\mathbf{I}_s(q-n) - \tilde{\mathbf{b}}^*(n)\mathbf{I}_c(q-n)) = \mathbf{F}_b(q).$$

The quantities $\tilde{\mathbf{a}}^*(n)$ and $\tilde{\mathbf{b}}^*(n)$ denote both the real $(\mathrm{Re}(\tilde{\mathbf{e}}^*(n)))$ and imaginary $(\mathrm{Im}(\tilde{\mathbf{e}}^*(n)))$ parts of transformation strain tensor $\tilde{\mathbf{e}}^*(n)$.

$\mathbf{F}_a(q)$ and $\mathbf{F}_b(q)$ denote:

$$\mathbf{F}_a(q) = \mathrm{Re}(F) = \mathbf{E}\mathbf{I}_c(q) - \mathbf{I}_{1c}^{\mathrm{p}}(q) + \frac{1}{|Y|}\sum_{n=-\infty}^{+\infty} R\ \mathbf{K}(n) : (\mathbf{I}_c^{\mathrm{p}}(n)\mathbf{I}_{cp}(q,n) - \mathbf{I}_s^{\mathrm{p}}(n)\mathbf{I}_{sm}(q,n))$$

$$\mathbf{F}_b(q) = -\mathrm{Im}(F) = \mathbf{E}\mathbf{I}_s(q) - \mathbf{I}_{1s}^{\mathrm{p}}(q) + \frac{1}{|Y|}\sum_{n=-\infty}^{+\infty} R\ \mathbf{K}(n) : (\mathbf{I}_c^{\mathrm{p}}(n)\mathbf{I}_{sp}(q,n) + \mathbf{I}_s^{\mathrm{p}}(n)\mathbf{I}_{cm}(q,n))$$

in which the integrals are given by

$$\mathbf{I}_c(q) = \int_{Y_1} \cos(2\pi Q\cdot y)\,\mathrm{d}y, \quad \mathbf{I}_s(q) = \int_{Y_1} \sin(2\pi Q\cdot y)\,\mathrm{d}y,$$

$$\mathbf{I}_{cp}(q,n) = \mathbf{I}_c(q-n) + \mathbf{I}_c(q+n), \quad \mathbf{I}_{cm}(q,n) = \mathbf{I}_c(q-n) - \mathbf{I}_c(q+n),$$

$$\mathbf{I}_{sp}(q,n) = \mathbf{I}_s(q-n) + \mathbf{I}_s(q+n), \quad \mathbf{I}_{sm}(q,n) = \mathbf{I}_s(q-n) - \mathbf{I}_s(q+n),$$

$$\mathbf{I}_c^{\mathrm{p}}(q) = \int_Y \mathbf{e}^{\mathrm{p}}(y)\cos(2\pi Q\cdot y)\,\mathrm{d}y, \quad \mathbf{I}_s^{\mathrm{p}}(q) = \int_Y \mathbf{e}^{\mathrm{p}}(y)\sin(2\pi Q\cdot y)\,\mathrm{d}y$$

$$\mathbf{I}_{1c}^{\mathrm{p}}(q) = \int_{Y_1} \mathbf{e}^{\mathrm{p}}(y)\cos(2\pi Q\cdot y)\,\mathrm{d}y, \quad \mathbf{I}_s^{\mathrm{p}}(q) = \int_{Y_1} \mathbf{e}^{\mathrm{p}}(y)\sin(2\pi Q\cdot y)\,\mathrm{d}y,$$

and the triple sum is defined as:

$$\sum_{n=-\infty}^{+\infty} R = \sum_{n_1=1}^{+\infty}\ \sum_{n_2=-\infty}^{+\infty}\ \sum_{n_3=-\infty}^{+\infty} + \sum_{\substack{n_2=1\\ n_1=0}}^{+\infty}\ \sum_{n_3=-\infty}^{+\infty} + \sum_{\substack{n_3=1\\ n_1=n_2=0}}^{+\infty}.$$

Owing to the symmetry considerations on $\tilde{\mathbf{a}}^*(n)$, $\tilde{\mathbf{b}}^*(n)$ and $\mathbf{K}(n)$ $(\tilde{\mathbf{a}}^*(n) = \tilde{\mathbf{a}}^*(-n)$, $\tilde{\mathbf{b}}^*(n) = -\tilde{\mathbf{b}}^*(-n)$ and $\mathbf{K}(n) = \mathbf{K}(-n))$, we can easily see that $\tilde{\mathbf{a}}^*(n)$ and $\mathbf{b}^*(n)$ are obtained in solving the following system of equations:

$$AP:\tilde{\mathbf{a}}^*(q)\,|\,Y\,| - \sum_{n=-\infty}^{+\infty} R\ \mathbf{K}(n):(\tilde{\mathbf{a}}^*(n)\mathbf{I}_{cp}(q,n)+\tilde{\mathbf{b}}^*(n)\mathbf{I}_{sm}(q,n)) = \mathbf{F}_a(q) \tag{19}$$

$$-AP:\tilde{\mathbf{b}}^*(q)\,|\,Y\,| - \sum_{n=-\infty}^{+\infty} R\ \mathbf{K}(n):(\tilde{\mathbf{a}}^*(n)\mathbf{I}_{sp}(q,n)-\tilde{\mathbf{b}}^*(n)\mathbf{I}_{cm}(q,n)) = \mathbf{F}_b(q) \tag{20}$$

In order to solve this system numerically, we truncate the infinite series after order $N_f$ and, therefore, the system of eqns (19) and (20) can be written with the matrix form:

$$\begin{array}{c} \\ 1 \\ N1(q) \\ N2(q) \end{array}\begin{array}{c} \begin{array}{ccc} 1 & N1(n) & N2(n) \end{array} \\ \begin{pmatrix} AP^{-1}\,|\,Y\,| & -\mathbf{K}(n)\mathbf{I}_{cp}(0,n) & -\mathbf{K}(n)\mathbf{I}_{sm}(0,n) \\ 0 & R1 & -\mathbf{K}(n)\mathbf{I}_{sm}(q,n) \\ 0 & -\mathbf{K}(n)\mathbf{I}_{sp}(q,n) & R2 \end{pmatrix} \end{array} \begin{pmatrix} \tilde{\mathbf{a}}^*(0) \\ \tilde{\mathbf{a}}^*(N1(q)) \\ \tilde{\mathbf{b}}^*(N2(q)) \end{pmatrix} = \begin{pmatrix} \mathbf{F}_a(0) \\ \mathbf{F}_a(q) \\ \mathbf{F}_b(q) \end{pmatrix},$$

where

$$R1 = AP\,|\,Y\,|\,\delta_{qn} - \mathbf{K}(n)\mathbf{I}_{cp}(q,n), \quad R2 = -AP\,|\,Y\,|\,\delta_{qn} + \mathbf{K}(n)\mathbf{I}_{cm}(q,n)$$

$$N1(n) = 2N_{eq}(n)-2, \quad N2(n) = 2N_{eq}(n)-1, \quad N_{eq}(n) = n_1(2N_f+1)^2+n_2(2N_f+1)+n_3+1.$$

## 3. HOMOGENIZED CONSTITUTIVE LAW

### 3.1. *Linear elastic behavior*

The relation between the macrostress and macrostrain tensors $(\mathbf{\Sigma}, \mathbf{E})$ is obtained by taking the mean value of formula (7) over $Y$ (the unit cell is not plasticized $\mathbf{e}^p(y) = 0$):

$$\mathbf{\Sigma} = \langle \boldsymbol{\sigma}(y) \rangle = a_2:(\mathbf{E} + \langle \mathbf{e}(\mathbf{v}(y)) \rangle - \langle \tilde{\mathbf{e}} \rangle). \tag{21}$$

The parentheses $\langle\ \rangle$ represents averaging over $Y$.

Since $\mathbf{v}(y)$ is periodic in $y$, one can see that $\langle \mathbf{e}(\mathbf{v}) \rangle = 0$, and, moreover, that $\langle \tilde{\mathbf{e}} \rangle = \tilde{\mathbf{e}}^*(0)$. Thus, the formula (21) becomes:

$$\mathbf{\Sigma} = a_2:(\mathbf{E} - \tilde{\mathbf{e}}^*(0)). \tag{22}$$

The eqn (22) can be rewritten as:

$$\mathbf{\Sigma} = a_2:(\mathbf{I}-\mathbf{B}):\mathbf{E}$$

where $\mathbf{I}$ denotes the fourth-order unit tensor.

We see that the stiffness homogenized tensor is expressed as:

$$a^{hom} = a_2:(\mathbf{I}-\mathbf{B}).$$

The fourth-order tensor $\mathbf{B}$ is defined by:

$$\mathbf{B}_{ijkh} = \tilde{\mathbf{e}}_{ij}^{*kh}(0)$$

$\tilde{\mathbf{e}}^{*kh}(0)$ is the solution of the system of eqns (19) and (20) for the elementary macrostrain $\mathbf{E}^{kh}$, which component $(i,j)$ is given by:

$$\mathbf{E}^{kh}_{ij} = \tfrac{1}{2}(\delta_{ih}\delta_{jk} + \delta_{ik}\delta_{jh}).$$

3.2. *Elastoplastic behavior*

The homogenized evolution law is described by an infinity of state variables which correspond to the microplastic strains over the unit cell (Suquet, 1987). Thus, Suquet (1983) suggests a simplified model by approximating the microplastic strain tensor ($\mathbf{e}^{\mathrm{p}}(y)$) with a constant inelastic microstrain within each subvolume ($Y^i$, $i = 1$ to $N_{\mathrm{v}}$), partitioning the unit cell into a finite number of subregions ($N_{\mathrm{v}}$). The internal variables now reduce to the finite set ($\mathbf{E}, \mathbf{e}^{\mathrm{p}}(y) = \mathbf{H}^i \, \forall y \in Y^i$). Furthermore, Hill's principle of maximum work, expressed at the microscopic level [ineqn (3)] and averaged over each subvolume $Y^i$, we can see that this principle holds also true for dual variables ($\Sigma^i, H^i$):

$$(\Sigma^i - \Sigma^{*i}) : \mathbf{H}^i \geqslant 0$$

$\Sigma^i \in DE$ and $\Sigma^{*i} \in DE$ using the convexity of the yield surface.

$\Sigma^i$ denotes the average of the microstress over the subvolume $Y^i\left(\langle \boldsymbol{\sigma} \rangle^i = \dfrac{1}{|Y^i|}\displaystyle\int_{Y^i} \boldsymbol{\sigma}\, \mathrm{d}Y\right)$.

Because of the equivalence between Hill's principle of maximum work and the normality rule, the evolution law of internal variables $\mathbf{H}^i$ is given by:

$$\begin{aligned}
&f^i_{\mathrm{c}}(y, \Sigma^i) < 0 && \Rightarrow \dot{\mathbf{H}}^i = 0\\
&f^i_{\mathrm{c}}(y, \Sigma^i) = 0 \quad \text{and} \quad \frac{\partial f^i_{\mathrm{c}}}{\partial \Sigma^i} : \dot{\Sigma}^i < 0 && \Rightarrow \dot{\mathbf{H}}^i = 0\\
&f^i_{\mathrm{c}}(y, \Sigma^i) = 0 \quad \text{and} \quad \frac{\partial f^i_{\mathrm{c}}}{\partial \Sigma^i} : \dot{\Sigma}^i = 0 && \Rightarrow \dot{\mathbf{H}}^i = \dot{\lambda}^i \frac{\partial f^i_{\mathrm{c}}}{\partial \Sigma^i} \quad \dot{\lambda}^i \geqslant 0,
\end{aligned} \tag{23}$$

where $f^i_{\mathrm{c}} = 0$ defines the equation of the yield convex surface.

This evolution law is integrated by using the set of the state variable $Z = (\mathbf{E}, \mathbf{H}^i, i = 1, N_{\mathrm{V}})$. To express $\Sigma^i$ as a function of $Z$, we take the average of formula (7) over $Y^i$:

$$\Sigma^i = a_2 : (\mathbf{E} + \langle \mathbf{e}(\mathbf{v}(Z)) \rangle^i - \mathbf{H}^i - \langle \tilde{\mathbf{e}}(Z) \rangle^i). \tag{24}$$

The expressions of $\langle \mathbf{e}(\mathbf{v}(Z)) \rangle^i$ and $\langle \tilde{\mathbf{e}}(Z) \rangle^i$ are given in Appendix B. The previous relation may be rewritten as (Pruchnicki and Shahrour, 1994):

$$\Sigma^i = S^i_{\mathrm{E}} : \mathbf{E} - \sum_j S^i_j : H^j. \tag{25}$$

Comparison between the eqns (24) and (25) gives the following result:

$$(S^i_E)_{khlm} = (a_2 : (\langle \mathbf{e}^{lm}(Z) \rangle^i + Z - \langle \tilde{\mathbf{e}}^{lm} \rangle^i))_{kh} \quad \text{for } Z = (\mathbf{E}^{lm}, 0) \tag{26}$$

$$(S^i_j)_{khlm} = (a_2 : (\langle \mathbf{e}^{lm}(Z) \rangle^i - Z - \langle \tilde{\mathbf{e}}^{lm} \rangle^i))_{kh} \quad \text{for } Z = (0, (\mathbf{H}^j)^{lm}) \tag{27}$$

where the component $(k, h)$ of the second-order tensor $(\mathbf{H}^j)^{lm}$ is defined by $1/2(\delta_{kl}\delta_{hm} + \delta_{km}\delta_{hl})$.

## 4. APPLICATION TO UNIDIRECTIONAL FIBER-REINFORCED COMPOSITES

### 4.1. *Simplification of the unit cell problem*

Consider a composite reinforced by continuous long fibers running parallel to the axial direction $y_1$ (Fig. 1). The geometry and the material properties of this medium are completely independent of the coordinate $y_1$ over the unit cell, therefore, $N_1$ is equal to zero in the Fourier series expansion.

As a result, one proves that the following components of $K$ vanish $K_{ijkh} = K_{khij} = 0$ when indices take the following values:

$$(i,j) = (1,2)(2,1)(1,3)(3,1)$$
$$(k,h) \neq (1,2)(2,1)(1,3)(3,1).$$

We define by $[(\tilde{a}^{kh})^*, (\tilde{b}^{kh})^*]$ the solution of the system of eqns (19) and (20), which get for the state variable $[Z = (\mathbf{E}^{kh}, 0)$ or $Z = (0, (\mathbf{H}^i)^{kh})]$. By using the particular form of tensor $\mathbf{K}(n)$ and the system mentioned above, we show that $((\tilde{a}^{ij}_{kh})^*, (\tilde{b}^{ij}_{kh})^*)$ and $((\tilde{a}^{kh}_{ij})^*, (\tilde{b}^{kh}_{ih})^*)$ are the solution of a linearly independent system of equations in which the second member is equal to zero.

Hence, we can express the following result:

$$\text{for } (l,m) = (1,1)(2,2)(3,3)(2,3)(3,2) \quad \text{and} \quad (i,j) = (1,2)(2,1)(1,3)(3,1)$$
$$(\tilde{a}^{lm}_{ij})^* = (\tilde{b}^{lm}_{ij})^* = 0$$
$$\text{for } (l,m) = (1,2)(2,1)(1,3)(3,1) \quad \text{and} \quad (i,j) = (1,1)(2,2)(3,3)(2,3)(3,2)$$
$$(\tilde{a}^{lm}_{ij})^* = (\tilde{b}^{lm}_{ij})^* = 0.$$

### 4.2. *Numerical elastic analysis*

We consider a ductile aluminum alloy matrix reinforced with circular cylindrical boron fibers. The fiber volume ratio is 50%. The elastic properties of the individual phases (fiber and matrix) used in the calculations are given in Table 1.

The coefficients of the system of eqns (19) and (20) are calculated with the integral given in Appendix C. The evolution of the homogenized stiffness are given in terms of the order of the Fourier series order ($N_f$) in Figs 2 and 3. We see that the homogenized components of stiffness tensor converge on an asymptotic value from fourth-order of the Fourier series. For the sake of simplicity, an idealized heterogeneous material with square fibers is associated to a real medium of circular fibers. The cross-sectional area of this associated medium is determined assuming the conservation of the fiber volume fraction. In Table 2, we report the ratio of the components of homogenized stiffness tensor of circular fibers composite to a square fibers one. A good agreement between the two different

Table 1. Constituent elastic constants for a boron fiber and an aluminum matrix

| | $E$ (MPa) Young's modulus | $\nu$ Poisson's ratio |
|---|---|---|
| Boron | $4\ 10^5$ | 0.2 |
| Aluminum | $7.5\ 10^4$ | 0.3 |

Table 2. Comparison between the elastic homogenized properties of a material of circular fibers and a square one

| $a_{1111}$ | $a_{2222}$ | $a_{1122}$ | $a_{2233}$ | $a_{1212}$ | $a_{2323}$ |
|---|---|---|---|---|---|
| 1 | 1 | 1 | 1.02 | 1 | 0.99 |

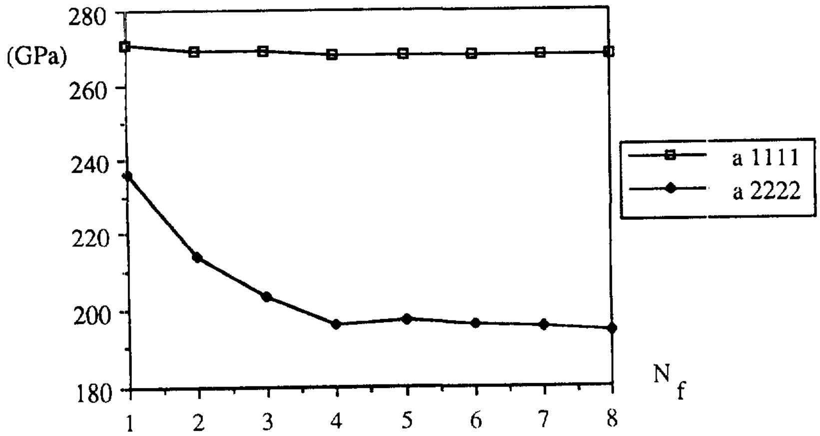


Fig. 2. Evolution of the components of elastic tensor in terms of the order of the Fourier series expansion.

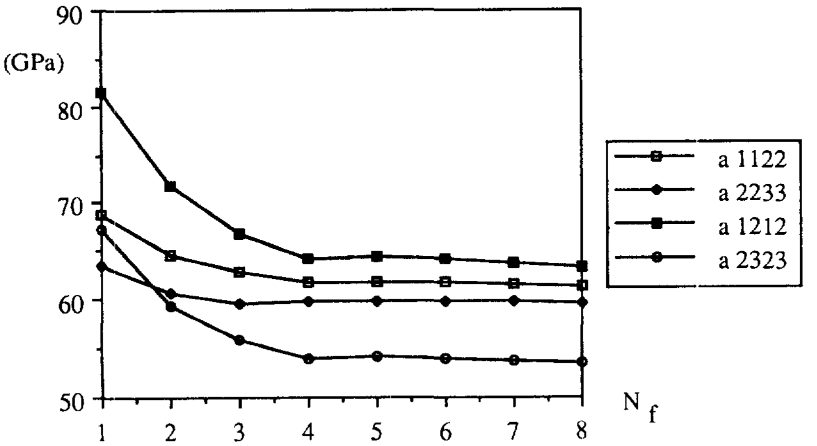


Fig. 3. Evolution of the components of elastic tensor in terms of the order of the Fourier series expansion.

modelings is found. As a result, the following computation is made with square fibers modeling the composite medium.

### 4.3. *Numerical elastic analysis using a simplified method*

Assuming that the inclusion phase undergoes a uniform microstrain, Suquet (1990) deduced a simplified expression of elastic homogenized tensor as:

$$\mathbf{a}_s^{\text{hom}} = a_2 + w_1(a_1 - a_2) : \left( \mathbf{I} + \frac{1}{|Y|^2 w_1} \sum_{n=-\infty}^{\infty}{}' \mathbf{H}(n) : (a_1 - a_2)\mathbf{I}(n)\mathbf{I}(-n) \right)^{-1}$$

where $w_1$ denotes the fiber volume fraction and the components of the fourth-order tensor $\mathbf{H}(n)(\mathbf{K}(n):(a_2)^{-1})$ are given by:

$$\mathbf{H}_{ijkh}(n) = \frac{1}{4\mu_2 \mathbf{N}^2}(N_i N_h \delta_{jk} + N_j N_h \delta_{ik} + N_i N_k \delta_{hj} + N_j N_k \delta_{hi}) - \frac{(\lambda_2 + \mu_2) N_i N_j N_k N_h}{\mu_2(\lambda_2 + 2\mu_2)\mathbf{N}^4}.$$

If $\mathbf{N} = \sqrt{N_i N_i}$ denotes the magnitude of the vector $\mathbf{N}$.

In comparison with the accurate method presented in the previous section, this approach avoids the technical difficulty associated with solving a linear system. In order to compare these elastic values with accurate ones, Suquet (1990) proved that if $(a_1 - a_2)$ is a positive definite form, therefore, $(a^{\text{hom}} - a_s^{\text{hom}})$ is also one. We now choose to apply this

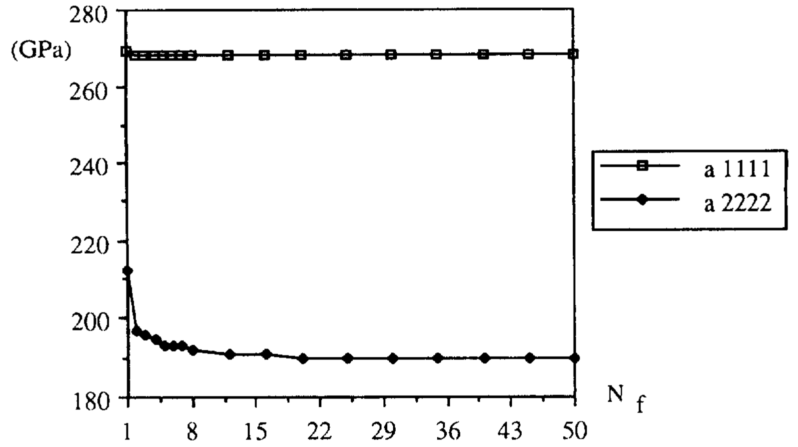


Fig. 4. Evolution of the components of simplified homogenized stiffness tensor in terms of the truncation order.

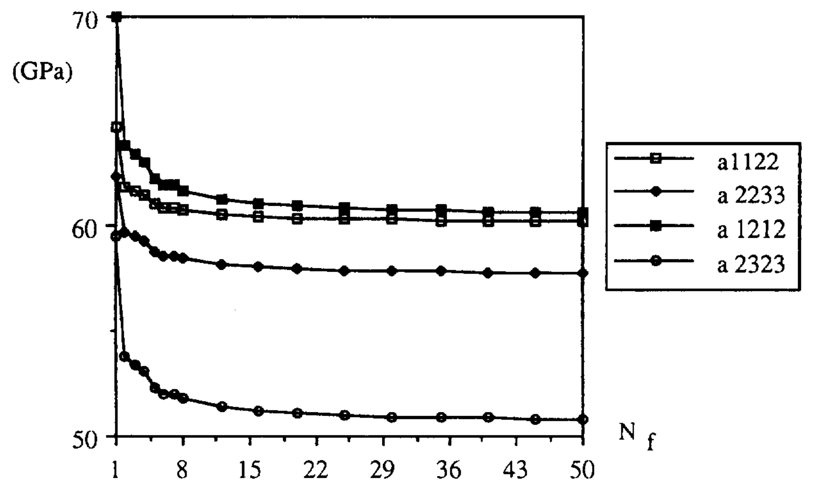


Fig. 5 Evolution of the components of simplified homogenized stiffness tensor in terms of the truncation order.

theory to the example studied in the previous section. The infinite sum has been truncated at order $N_f$. In Figs 4 and 5, we see that the components of elastic homogenized tensor converge on an asymptotic value when the truncation order increases. The numerical value obtained at the truncation order 50 is carried. In Table 3, we report the ratio of the components of accurate stiffness elastic tensor to a simplified one. An examination of these numerical results reveals that the simplified theory provides an excellent estimate. We can also verify that the two quantities $(a_1 - a_2)$ and $(a^{hom} - a_s^{hom})$ are positive definite forms.

Finally, it is important to note that the range of validity of such a method is the elasticity. The main reason is the uniformity of the strain tensor within the inclusion which implies considering the same hypothesis on plastic strain and this assumption may be too simple for describing the hardening of composite materials (Dvorak, 1991; Accorsi and Nemat-Nasser, 1986; Walker *et al.*, 1993; Moulinec and Suquet, 1994).

Table 3. Comparison between accurate elastic homogenized properties and simplified ones

| $a_{1111}$ | $a_{2222}$ | $a_{1122}$ | $a_{2233}$ | $a_{1212}$ | $a_{2323}$ |
|---|---|---|---|---|---|
| 1 | 1.03 | 1.02 | 1.02 | 1.05 | 1.05 |

### 4.4. *Elastoplastic behavior*

4.4.1. *Procedure of integration.* The macrobehavior of the homogenized material has been investigated on imposed macrostrain paths. The integration can be constructed by determining the rate of state variables resulting from the one of macrostrain. Averaging incremental relation (7) over $Y$, we have finally:

$$a^{\text{hom}} : \Delta\mathbf{E} - a_2 : \frac{1}{|Y|}\sum_j \Delta\mathbf{H}^j \,|\, Y^j \,| = \Delta\Sigma. \tag{28}$$

Taking into account formula (25), the consistency condition for plastified material is expressed as:

$$\Delta\mathbf{E} : \frac{\partial f_c^i}{\partial \boldsymbol{\Sigma}^i} : \mathbf{S}_E^i + \sum_j \Delta\mathbf{H}^j : \frac{\partial f_c^i}{\partial \boldsymbol{\Sigma}^i} : \mathbf{S}_j^i = 0. \tag{29}$$

From formulas (23), (28) and (29), we can establish the system of equations which allows us to compute the incremental unknown $(\Delta\mathbf{E}, \Delta\lambda^i)$ at each increment of macrostrain loading $(\Delta\Sigma)$:

$$\mathbf{M}\begin{pmatrix} \Delta\mathbf{E} \\ \Delta\lambda^j \end{pmatrix} = \begin{pmatrix} \Delta\Sigma \\ 0 \end{pmatrix}$$

where $\mathbf{M}$ is the matrix defined by:

$$\begin{array}{c} \\ 1 \\ \\ i \end{array} \begin{array}{c} \begin{array}{cc} \quad 1 \quad & \quad j \quad \end{array} \\ \begin{bmatrix} a^{\text{hom}} & -\dfrac{|Y^j| a_2}{|Y|} : \dfrac{\partial f_c^j}{\partial \boldsymbol{\Sigma}^j} \\ \dfrac{\partial f_c^i}{\partial \boldsymbol{\Sigma}^i} : \mathbf{S}_E^i & \dfrac{\partial f_c^i}{\partial \boldsymbol{\Sigma}^i} : \dfrac{\partial f_c^i}{\partial \boldsymbol{\Sigma}^j} : \mathbf{S}_j^i \end{bmatrix} \end{array}.$$

For constant plastification over a rectangular subregion the determination of the tensor $\mathbf{S}_E^i$ and $\mathbf{S}_j^i$, which is defined by eqns (26) and (27), requires computation of the integrals given in Appendix C.

In order to keep the microstress state of plastified material on yield surface, the microplastic strain has been corrected by using a Taylor development at first-order (iteration $k$):

$$f_c^i(\boldsymbol{\Sigma}^i(k)) = f_c^i(\boldsymbol{\Sigma}^i(k-1) + \Delta\boldsymbol{\Sigma}^i(k)) = f_c^i(\boldsymbol{\Sigma}^i(k-1)) + \frac{\partial f_c^i}{\partial \boldsymbol{\Sigma}^i}(\boldsymbol{\Sigma}^i(k-1)) : \Delta\boldsymbol{\Sigma}^i(k) = 0.$$

As a result, the state variable has been determined by solving, in an iterative process, the following system of equations:

$$\mathbf{M}(k-1)\begin{pmatrix} \Delta\mathbf{E} \\ \Delta\lambda^j \end{pmatrix} = \begin{pmatrix} 0 \\ -f_c(\boldsymbol{\Sigma}^i(k-1)) \end{pmatrix}.$$

4.4.2. *Numerical simulations.* The unit cells of both the square and circular fiber

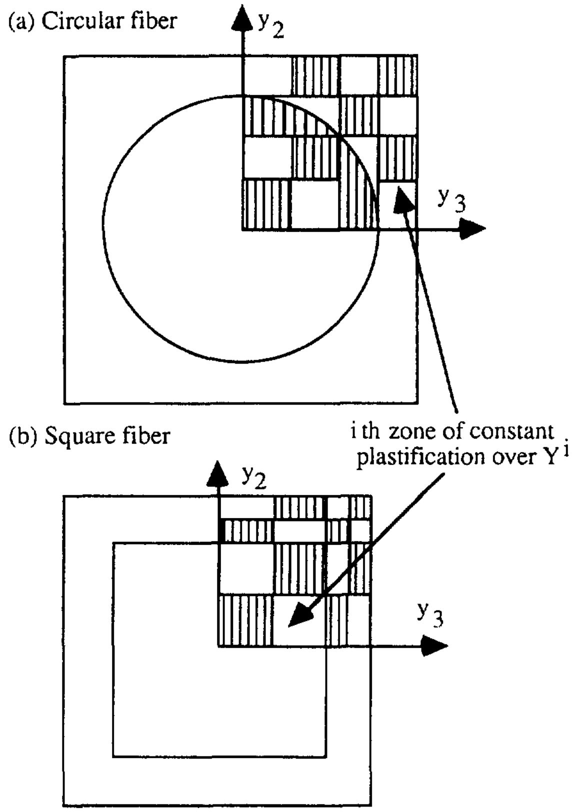


Fig. 6. Unit cell divided into 64 zones of constant plastification: (a) square fiber; (b) circular fiber.

composites are divided into sixty four areas of constant plastification (Fig. 6). Assuming that both the boron and aluminum satisfy the elastic-perfectly plastic Von Mises law the yield criterion of which takes the form:

$$f_c^i = [\tfrac{1}{2}((\sigma_{11}-\sigma_{22})^2+(\sigma_{11}-\sigma_{33})^2+(\sigma_{22}-\sigma_{33})^2)+3(\sigma_{12}^2+\sigma_{13}^2+\sigma_{23}^2)]^{1/2}-\bar{\sigma}_t^i$$

where $\bar{\sigma}_t^i$ $(i = 1, 2)$ denotes the elasticity limit in simple tension of fiber $(i = 1)$ and matrix $(i = 2)$, the numerical values of which are equal to 3400 and 450 MPa, respectively. The composite material has been subjected to simple macrotension ($\Sigma 1$) in the plane $(y_1, y_2)$. Let $\alpha\Sigma(=(y_1, \Sigma 1))$ denote the angle between both the fibers $y_1$-axis and the macrotension ($\Sigma 1$).

For, respectively, square and circular fibers, Figs 7 and 8 show the evolution of the macrostress tensor of seven tension paths in different directions with the $y_1$-axis ($\alpha\Sigma = 0, 15, 30, 45, 60, 75$ and $90^\circ$) in terms of the equivalent macrostrain: $\mathbf{EQ} = (\mathbf{E}_{ij}\mathbf{E}_{ij})^{0.5}$. It can be observed that, for each path, the macro response involves three phases. The initial elastic phase is followed by a plastic phase with nonlinear hardening and decreasing stiffness. The last phase corresponds to perfect plastification. We can see that the macrofailure depends on the direction of the loading.

The agreement between the nonlinear response of both circular and square fibers composites is good. The hardening of the circular fiber composite is more important than the corresponding one of square fiber for the off-axis uniaxial tension comprising between 75 and $90^\circ$. In Fig. 11, we see that the square fiber composite overestimates slightly the initial elasticity limit. On the contrary, for failure the results between circular and square fibers are in excellent agreement for direction of simple tension orientated at an angle up to $75^\circ$ to the fiber axis. Nevertheless, for the remaining loading direction ($75^\circ \leqslant \alpha\Sigma \leqslant 90^\circ$) the square fiber composite predicts slightly higher failure stresses compared to those given by the circular fiber model.

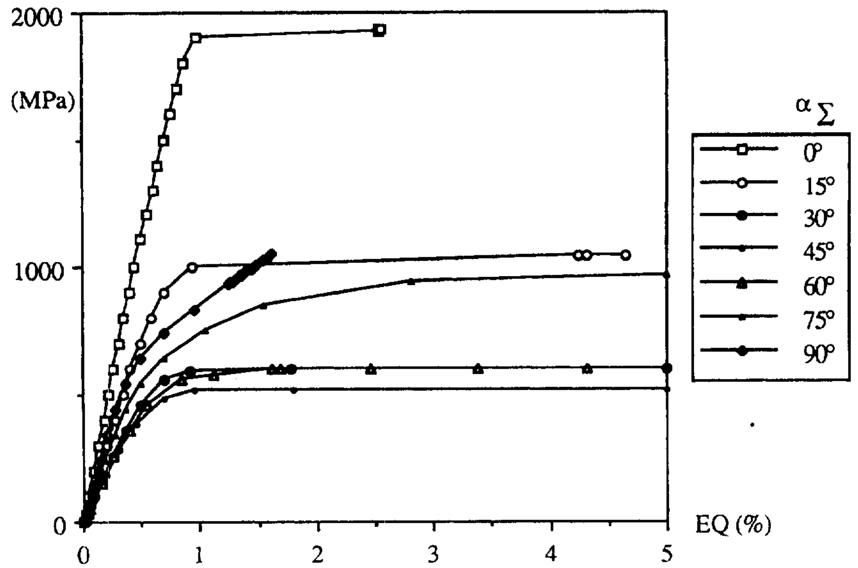


Fig. 7. Macroscopic uniaxial stress–strain response of homogenized aluminum/boron circular fiber composite.

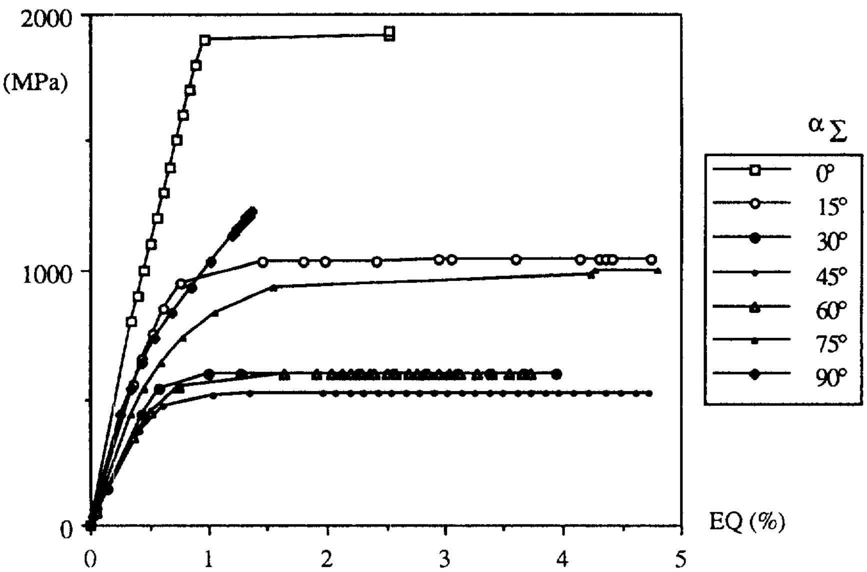


Fig. 8. Macroscopic uniaxial stress–strain response of homogenized aluminum/boron square fiber composite.

4.4.3. *Inelastic behavior of laminated media.* This section is devoted to the study of periodic stratified composites of which the unit cell is illustrated in Fig. 9. This type of composite material presents a great interest both in engineering as well as in mathematics literature (Salamon, 1968; Sawicki, 1981; Auriault and Bonnet, 1985; Papamichos *et al.*, 1990; Boutin, 1996). For loading path in simple tension defined previously, we will investigate the mechanical performances of the geometrical arrangement of phases in comparison with the fibrous one. Thus, the multilayered material is defined in the following way, the mechanical properties and the volume fraction of each constituent are chosen to be the same as the ones of the fiber composite material. Fig. 10 shows that the simple tension evolution law of this multilayered material is in good agreement with the corresponding one of fiber composite (Figs 7 and 8) except for simple tension in plane transverse to the fiber axis ($\alpha\Sigma = 90°$). The reason is that the failure load for the multilayered material is approximately twice as high as that of the fiber material (Fig. 11). Moreover, we verify in

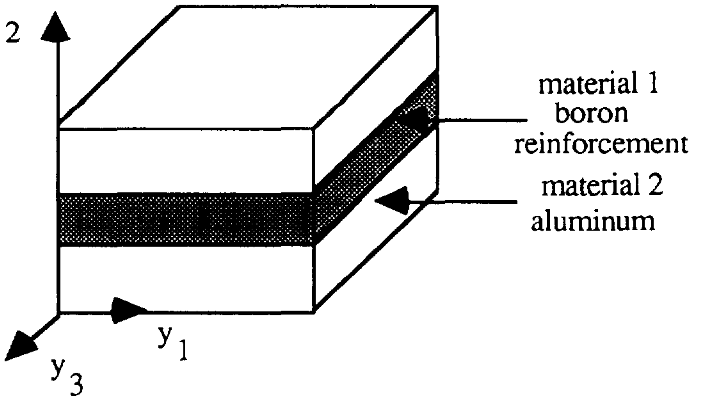


Fig. 9. Unit cell of the multilayered material.

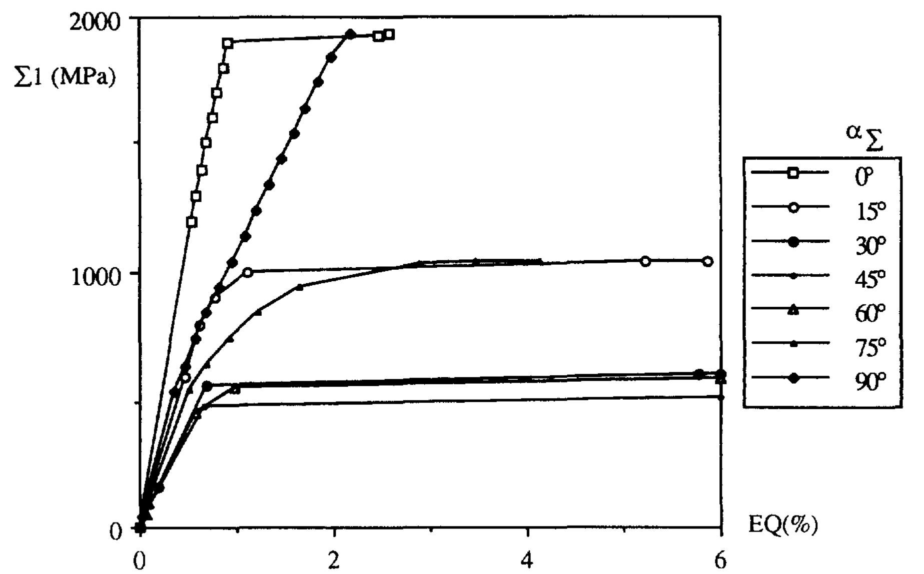


Fig. 10. Macroscopic uniaxial stress–strain response of homogenized aluminum/boron multilayered composite.

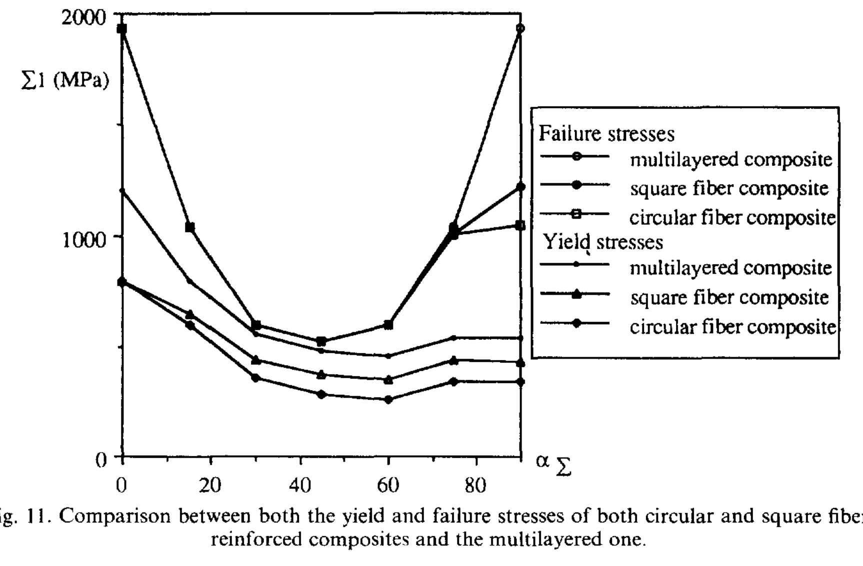


Fig. 11. Comparison between both the yield and failure stresses of both circular and square fiber-reinforced composites and the multilayered one.

Fig. 11 that the failure macrostresses in simple uniaxial tensions in parallel and perpendicular directions with the stratification are equal to the mean value of the simple failure tensions of each constituent. This result is proved rigorously in Appendix D. Finally, we can observe that the elasticity limit is slightly smaller for fiber material than for multilayered.

## 5. CONCLUSION

This paper presents an approximate elastoplastic homogenized law described by a finite number of state variables. An integral equation approach is used to determine microstress and microstrain at any point in the unit cell. The integral equation is solved by a Fourier series expansion of the microfield variables. A numerical study on a metal–matrix composite reveals that the elastic homogenized components converge on an asymptotic value with increasing order of the Fourier series expansion. The macroscopic elastoplastic homogenized law is explored over tension loading paths in plane containing the fibers. A significant and important anisotropic hardening can be observed. The effect of the shape of the fiber is noticeable on the hardening behavior in the plane transverse to fiber axis.

Work is now in progress to take into consideration interface conditions between the two constituents, enabling one to improve the description of the behavior of composite material.

## REFERENCES


Aboudi, J. (1986) *Elastoplasticity Theory for Composite Materials*. SM Archives, Oxford University Press, England, pp. 141–183.

Aboudi, J. (1991) *Mechanics of Composite Materials—A Unified Macromechanical Approach*. Elsevier, Amsterdam.

Accorsi, M. L. and Nemat-Nasser, S. (1986) Bounds on the overall elastic and instantaneous elastoplastic moduli of periodic composites. *Mechanics of Materials* **5**, 209–220.

Auriault, J. L. and Bonnet, G. (1985) Dynamique des composites élastiques. *Archives of Mechanics* **37**, 269–284.

Bensoussan, A., Lions, J.-L. and Papanicolaou, G. (1978) *Asymptotic Analysis for Periodic Structures Studies in Mathematics and its Applications*. North Holland, Amsterdam.

Boutin, C. (1996) Microstructural effects in elastic composites. *International Journal of Solids and Structures* **33**, 1025–1051.

Devries, F., Dumontet, H., Duvaut, G. and Lene, F. (1989) Homogenization and damage for composite structures. *International Journal for Numerical Methods in Engineering* **27**, 285–298.

Dumontet, H. (1983) Homogénéisation par développements en séries de Fourier. *Comptes Rendus de l'Académie des Sciences, Paris* **296**(II), 1625–1628.

Dvorak, G. J. (1991) Plasticity theories for fibrous composite materials. In *Metal Matrix Composites: Mechanisms and Properties*, eds R. K. Everett and R. J. Arsenault. Academic Press, Boston, pp. 1–77.

Ghosh, S., Lee, K. and Moorthy, S. (1995) Multiple scale analysis of heterogeneous elastic structures using homogenization theory and voronoi cell finite element method. *International Journal of Solids and Structures* **32**, 27–62.

Guedes, J. M. (1990) Nonlinear computational model for composite material using homogenization. Ph.D. dissertation, University of Michigan, MI.

Guedes, J. M. and Kikuchi, N. (1991) Preprocessing and postprocessing for materials based on the homogenization method with adaptive finite elements methods. *Computer Methods in Applied Mechanics and Engineering* **83**, 143–198.

Halpen, B. and Nguyen, Q. S. (1975) Sur les matériaux standards généralisés. *Journal de Mécanique* **14**(1), 39–63.

Iwakuma, T. and Nemat-Nasser, S. (1983) Composite with periodic microstructure. *Computers and Structures* **16**(1–4), 13–19.

Jansson, S. (1992) Homogenized non linear constitutive properties and local stress concentrations for composites with periodic internal structure. *International Journal of Solids and Structures* **29**, 2181–2200.

Kröner, E. (1972) *Statistical Continuum Mechanics*. Springer, Wien, p. 110.

Lene, F. (1987) Contribution to the study of composite materials and their damage. Translation of thesis presented to Université Pierre et Marie Curie, Paris VI, Technical translation report, NASA TT-20107.

Moulinec, H. and Suquet, P. (1994) A fast numerical method for computing the linear and nonlinear mechanical properties of composites. *Comptes Rendus de l'Académie des Sciences, Paris* **318**(II), 1417–1423.

Nemat-Nasser, S. and Taya, M. (1981) On effective moduli of an elastic body containing $y$ periodically distributed voids. *Quarterly of Applied Mathematics* April 1981, 43–59.

Nemat-Nasser, S., Iwakuma, T. and Hejazi, M. (1982) On composites with periodic structure. *Mechanics of Materials* **1**, 239–267.

Nemat-Nasser, S. and Taya, M. (1985) On effective moduli of an elastic body containing $y$ periodically distributed voids: comments and corrections. *Quarterly of Applied Mathematics* **39**, 187–189.

Nemat-Nasser, S., Iwakuma, T. and Accorsi, M. (1986) Cavity growth and grain boundary sliding in polycrystalline solids. *Mechanics of Materials* **5**, 317–329.

Nemat-Nasser, S., Yu, N. and Hori, M. (1993) Solids with periodically distributed cracks. *International Journal of Solids and Structures* **30**, 2071–2095.

Papamichos, E., Vardoulakis, I. and Mülhaus, H. B. (1990) Buckling of layered media: a Cosserat-continuum approach and its validation. *International Journal for Numerical and Analytical Methods in Geomechanics* **14**, 473–498.

Pruchnicki, E. and Shahrour, I. (1992) Loi d'évolution homogénéisée du matériau multicouche à constituants élastoplastiques parfaits. *Comptes Rendus de l'Académie des Sciences, Paris* **315**(II), 137–142.

Pruchnicki, E. and Shahrour, I. (1993) Etude des caractéristiques homogénéisés d'un matériau composite à comportement élastoplastique à l'aide d'un programme utilisant les développements en séries de Fourier. *Actes des Conférences*, Strucome, vol. 93, pp. 387–398.

Pruchnicki, E. and Shahrour, I. (1994) A macroscopic elastoplastic constitutive law for multilayered media: application to reinforced earth material. *International Journal for Numerical and Analytical Methods in Geomechanics* **18**, 507–518.

Pruchnicki, E. (1996) Sur quelques aspects de la théorie de l'homogénéisation des milieux périodiques. Habilitation à diriger des recherches, University of Lille. Submitted.

Sanchez-Palencia, E. (1980) *Non-homogeneous Media and Vibration Theory Lectures Notes in Physics*. Springer, Berlin.

Salamon, M. D. G. (1968) Elastic moduli of a stratified rock mass. *International Journal of Rock Mechanics and Mining Sciences and Geomechanics* **5**, 519–527.

Sawicki, A. (1981) Yield condition for layered composites. *International Journal of Solids and Structures* **17**, 969–979.

Suquet, P. (1987) Elements of homogenization for inelastic solid mechanics. In *Homogenization Techniques for Composite Media, Lecture Notes in Physics*, eds E. Sanchez Palencia and A. Zaoui, No. 272. Springer, Berlin, pp. 193–278.

Suquet, P. (1983) Local and global aspects in the mathematical theory of plasticity. *Plasticity Today Symposium*, Udine, pp. 279–310.

Suquet, P. (1990) Une méthode simplifée pour le calcul des propriétés élastiques de matériaux hétérogènes à structure périodique. *Comptes Rendus de l'Académie des Sciences, Paris* **311**(II), 769–774.

Toledano, A. and Murakami, H. (1987) A high-order mixture model for periodic particulate composites. *International Journal of Solids and Structures* **23**, 989–1002.

Walker, K. P., Jordan, E. H. and Freed, A. D. (1990) Equivalence of Green's functions and the Fourier series representation of composites with periodic microstructure. In *Micromechanics and Inhomogeneity*, The Toshio Mura Anniversary Volume, eds G. J. Weng, M. Taya and H. Abé, pp. 535–558. Springer, New York.

Walker, K. P., Jordan, E. H. and Freed, A. D. (1991) Microstress analysis of periodic composites. *Composites Engineering* **1**(1), 29–40.

Walker, K. P., Jordan, E. H. and Freed, A. D. (1993) Thermoplastic analysis of fibrous periodic composites using triangular subvolumes. NASA TM 106076. NASA-Lewis Research Center, Cleveland, OH.

## APPENDIX A

*Calculation of tensor* $\boldsymbol{K}$

Equations (8)–(10) lead to:

$$\mathbf{e}^*_{kh}(n) = i\pi(\mathbf{N}_k\mathbf{v}^*_h(n) + \mathbf{N}_h\mathbf{v}^*_k(n)). \tag{A1}$$

The equilibrium equations (1), the constitutive law (7), and the Fourier series expansion (10)–(12) show that:

$$(a_2)_{ijkh}\mathbf{N}_j\mathbf{e}^*_{kh}(n) = (a_2)_{ijkh}\mathbf{N}_j(\tilde{\mathbf{e}}^*_{kh}(n) + \mathbf{e}^{p*}_{kh}(n)). \tag{A2}$$

Taking into account the elastic linear behavior of the matrix, eqn (A2) becomes:

$$2i\pi[(\lambda_2+\mu_2)\mathbf{N}_i\mathbf{N}_h\mathbf{v}^*_h(n) + \mu_2\mathbf{N}^2\mathbf{v}^*_i(n)] = (\lambda_2\mathbf{N}_i\delta_{kh} + \mu_2\mathbf{L}_{ikh})(\tilde{\mathbf{e}}^*_{kh}(n) + \mathbf{e}^{p*}_{kh}(n)) \tag{A3}$$

with $\mathbf{N}^2 = \mathbf{N}_1^2 + \mathbf{N}_2^2 + \mathbf{N}_3^2$ and $\mathbf{L}_{ikh} = \delta_{ih}\mathbf{N}_k + \delta_{ik}\mathbf{N}_h$. By multiplying both sides of this relation by $\mathbf{N}_h$, we get:

$$\mathbf{N}_h\mathbf{v}^*_h(n) = \frac{1}{i\pi(\lambda_2+2\mu_2)}\left[\frac{\lambda_2\delta_{kh}}{2} + \frac{\mu_2\mathbf{N}_k\mathbf{N}_h}{\mathbf{N}^2}\right](\tilde{\mathbf{e}}^*_{kh}(n) + \mathbf{e}^{p*}_{kh}(n)).$$

Substituting this relation into (A3) provides:

$$\mathbf{v}^*_i(n) = \frac{1}{i\pi}\left[\frac{1}{2\mathbf{N}^2}\mathbf{L}_{ikh} + \frac{\lambda_2\mathbf{N}_i\delta_{kh}}{2\mu_2\mathbf{N}^2} - \frac{(\lambda_2+\mu_2)\mathbf{N}_i}{(\lambda_2+2\mu_2)\mathbf{N}^2}\left(\frac{\lambda_2}{2\mu_2}\delta_{kh} + \frac{\mathbf{N}_k\mathbf{N}_h}{\mathbf{N}^2}\right)\right](\tilde{\mathbf{e}}^*_{kh}(n) + \tilde{\mathbf{e}}^{p*}_{kh}(n)). \tag{A4}$$

Using eqns (A1) and (A4) yields the components of the fourth-order tensor $\mathbf{K}$:

$$\mathbf{K}_{ijkh}(n) = \frac{1}{2\mathbf{N}^2}(\mathbf{N}_j\mathbf{L}_{ikh} + \mathbf{N}_i\mathbf{L}_{jkh}) - \frac{2(\lambda_2+\mu_2)\mathbf{N}_i\mathbf{N}_j\mathbf{N}_k\mathbf{N}_h}{(\lambda_2+2\mu_2)\mathbf{N}^4} + \frac{\lambda_2\mathbf{N}_i\mathbf{N}_j\delta_{kh}}{(\lambda_2+2\mu_2)\mathbf{N}^2}.$$

## APPENDIX B

*Determination of* $\langle \tilde{\mathbf{e}} \rangle^i$

It follows from eqn (11) that:

$$\tilde{\mathbf{e}}(y) = \sum_{n=-\infty}^{+\infty} (\tilde{\mathbf{a}}^*(n) + i\tilde{\mathbf{b}}^*(n))\, e^{2\pi i N \cdot y}.$$

This equation may be rewritten as:

$$\tilde{\mathbf{e}}(y) = \tilde{\mathbf{a}}^*(0) + 2 \sum_{n=-\infty}^{+\infty}{}^{R} (\tilde{\mathbf{a}}^*(n)\cos(2\pi\mathbf{N}\cdot y) - \tilde{\mathbf{b}}^*(n)\sin(2\pi\mathbf{N}\cdot y)).$$

By averaging this relation over $Y^i$, we get:

$$\langle \tilde{\mathbf{e}} \rangle^i = \tilde{\mathbf{a}}^*(0) + \frac{2}{|Y^i|} \sum_{n=-\infty}^{+\infty}{}^{R} (\tilde{\mathbf{a}}^*(n)\mathbf{I}_c^i(n) - \tilde{\mathbf{b}}^*(n)\mathbf{I}_s^i(n))$$

where

$$\mathbf{I}_c^i(n) = \int_{Y^i} \cos(2\pi\mathbf{N}\cdot y)\, dy, \quad \mathbf{I}_s^i(n) = \int_{Y^i} \sin(2\pi\mathbf{N}\cdot y)\, dy.$$

*Determination of* $\langle \mathbf{e} \rangle^i$

Using eqn (10) in conjunction with formula (15), it becomes:

$$\mathbf{e}(\mathbf{v}(y)) = \sum_{n=-\infty}^{+\infty}{}' \mathbf{K}(n):(\tilde{\mathbf{e}}^*(n) + \tilde{\mathbf{e}}^{p*}(n))\, e^{2\pi i \mathbf{N}\cdot y}. \tag{B1}$$

Considering that the state of plastification is described by a finite number of variables ($\mathbf{H}^j$), eqn (14) becomes:

$$\tilde{\mathbf{e}}^{p*}(n) = \frac{1}{|Y|} \sum_j \mathbf{H}^j(\mathbf{I}_c^j(n) - i\mathbf{I}_s^j(n)). \tag{B2}$$

Substituting eqn (B2) into formula (B1), we get:

$$\mathbf{e}(\mathbf{v}(y)) = 2 \sum_{n=-\infty}^{+\infty}{}^{R} (\tilde{\mathbf{A}}^*(n)\cos(2\pi\mathbf{N}y) - \tilde{\mathbf{B}}^*(n)\sin(2\pi\mathbf{N}y))$$

where

$$\tilde{\mathbf{A}}^*(n) = \mathbf{K}(n):\left(\tilde{\mathbf{a}}^*(n) + \frac{1}{|Y|}\sum_j \mathbf{H}^j\mathbf{I}_c^j(n)\right)$$

$$\tilde{\mathbf{B}}(n) = \mathbf{K}(n):\left(\tilde{\mathbf{b}}^*(n) - \frac{1}{|Y|}\sum_j \mathbf{H}^j\mathbf{I}_s^j(n)\right)$$

Averaging the previous relation over $Y^i$ yields the final relation:

$$\langle \mathbf{e}(\mathbf{v}(y)) \rangle^i = \frac{1}{|Y|} \sum_{n=-\infty}^{+\infty}{}^{R} (\tilde{\mathbf{A}}^*(n)\mathbf{I}_c^i(n) - \tilde{\mathbf{B}}^*(n)\mathbf{I}_s^i(n)).$$

## APPENDIX C

*Some explicit forms of I integral*

Calculation of $I(q)$

*Rectangular cylindrical area* $Y^i$

$d_{2i}$ and $d_{3i}$ are the dimensions of a rectangle, with the center located at the point of coordinates $(y_{2i}, y_{3i})$.

(Case 1) $q_2 \neq 0$ and $q_3 \neq 0$ $\quad \mathbf{I}(q) = \dfrac{\sin(\pi Q_2 d_{i2})\sin(\pi Q_3 d_{i3})}{\pi^2 Q_2 Q_3} e^{-2i\pi(Q_2 y_{2i} + Q_3 y_{3i})}.$

(Case 2) $q_2 = 0$ and $q_3 \neq 0$ $\quad \mathbf{I}(q) = d_{i2}\dfrac{\sin(\pi Q_3 d_{i3})}{\pi Q_3} e^{-2i\pi Q_3 y_{3i}}.$

(Case 3) $q_2 \neq 0$ and $q_3 = 0$ $\quad \mathbf{I}(q) = d_{i3}\dfrac{\sin(\pi Q_2 d_{i2})}{\pi Q_2} e^{-2i\pi Q_2 y_{2i}}.$

(Case 4) $q_2 = 0$ and $q_3 = 0$ $\quad \mathbf{I}(q) = \pi d_{i2} d_{i3}.$

*Circular cylindrical area centered at the origin*
$d$ and $R$ stand for the dimensions of the unit cell and the radius of the cross-section of the fiber.

$$\text{(Case 1) } q \neq 0 \quad \mathbf{I}(q) = \frac{J(X_1)}{X_2} \quad \text{with } X_1 = \frac{2\pi R}{d}(q_1^2+q_2^2)^{1/2} \quad \text{and} \quad X_2 = \frac{1}{\mathrm{d}R}(q_1^2+q_2^2)^{1/2}.$$

$$\text{(Case 2) } q = 0 \quad \mathbf{I}(q) = \pi R^2.$$

$J$ denotes the Bessel function.

## APPENDIX D

*Failure of the homogenized multilayered material in directions parallel and perpendicular to stratification*

For the multilayered material, the microstress tensor is constant in each constituent (Sawicki, 1981; Pruchnicki and Shahrour, 1993). As a consequence of this result, the macrostress tensor can be expressed as a function of the micro one in the simplified way:

$$\Sigma = \sum_{\alpha} w_\alpha \boldsymbol{\sigma}^\alpha \tag{D1}$$

where $\boldsymbol{\sigma}^\alpha$ and $w_\alpha$ designate, respectively, the microstress tensor and the volume fraction in the $\alpha$th constituent.

*Tension path along* $y_1$ *axis*. The multilayered material is subjected to a single tension in direction parallel to stratification. The relations linking the macrostress and microstress tensors (D1) becomes:

$$\Sigma_1 = w_1\boldsymbol{\sigma}_{11}^1 + w_2\sigma_{11}^2 \tag{D2}$$

$$\Sigma_{22} = \boldsymbol{\sigma}_{22}^1 = \boldsymbol{\sigma}_{22}^2 = 0 \tag{D3}$$

$$\Sigma_{33} = w_1\sigma_{33}^1 + w_2\boldsymbol{\sigma}_{33}^2 = 0 \tag{D4}$$

$$\Sigma_{12} = \boldsymbol{\sigma}_{12}^1\boldsymbol{\sigma}_{12}^2 = 0 \tag{D5}$$

$$\Sigma_{13} = w_1\boldsymbol{\sigma}_{13}^1 + w_2\boldsymbol{\sigma}_{13}^2 = 0 \tag{D6}$$

$$\Sigma_{23} = \boldsymbol{\sigma}_{23}^1 = \boldsymbol{\sigma}_{23}^2 = 0. \tag{D7}$$

With the help of eqns (D3), (D5) and (D7), we see that the Von Mises yield criterion is expressed in the $\alpha$th constituent as follows:

$$(\boldsymbol{\sigma}_{11}^\alpha)^2 + (\boldsymbol{\sigma}_{11}^\alpha - \boldsymbol{\sigma}_{33}^\alpha)^2 + (\boldsymbol{\sigma}_{33}^\alpha)^2 + 6(\boldsymbol{\sigma}_{13}^\alpha)^2 \leqslant 2(\bar{\boldsymbol{\sigma}}_t^\alpha)^2. \tag{D8}$$

This inequality can be rewritten in the form:

$$-\sqrt{B_\sigma^\alpha} \leqslant \boldsymbol{\sigma}_{11}^\alpha - \boldsymbol{\sigma}_{33}^\alpha \leqslant \sqrt{B_\sigma^\alpha}$$

$B_\sigma^\alpha$ denotes $2(\bar{\boldsymbol{\sigma}}_t^\alpha)^2 - (\boldsymbol{\sigma}_{11}^\alpha)^2 - (A_\sigma^\alpha)^2$ by setting $(A_\sigma^\alpha)^2 = (\boldsymbol{\sigma}_{33}^\alpha)^2 + 6(\boldsymbol{\sigma}_{13}^\alpha)^2$.

We multiply each part of the previous inequalities by the volume fraction of $\alpha$th constituent and we sum them. By taking into account formulas (D2) and (D4), we obtain an upper bound of $\Sigma 1$:

$$\Sigma 1 \leqslant B_{\mathrm{M}} \text{ with } B_{\mathrm{M}} = w_1\sqrt{B_\sigma^1} + w_2\sqrt{B_\sigma^2}.$$

The eqns (D4) and (D6) allow us to show that:

$$(A_\sigma^2)^2 = \left(\frac{w_1}{w_2}\right)^2 (A_\sigma^1)^2.$$

As a consequence the upper bound $B_{\mathrm{M}}$ can be written in the form:

$$B_{\mathrm{M}} = w_1\sqrt{2(\bar{\boldsymbol{\sigma}}_t^1)^2 - (\boldsymbol{\sigma}_{11}^1)^2 - (A_\sigma^1)^2} + w_2\sqrt{2(\bar{\boldsymbol{\sigma}}_t^2)^2 - (\boldsymbol{\sigma}_{11}^2)^2 - \left(\frac{w_1}{w_2}A_\sigma^1\right)^2}.$$

In considering $A_\sigma^1$ as a variable, we propose to seek a maximal value of this upper bound. Then we calculate the partial derivative of the upper bound $B_{\mathrm{M}}$ with respect to $A_\sigma^1$.

$$\frac{\partial B_M}{\partial A_\sigma^1} = -2A_\sigma^1\left(\frac{1}{\sqrt{B_\sigma^1}} + \left(\frac{w_1}{w_2}\right)^2 \frac{1}{\sqrt{B_\sigma^2}}\right)$$

We see that the upper bound $B_M$ attains a maxima when $A_\sigma^1 = 0$ and, consequently, $\sigma_{33}^1 = 0$ and $\boldsymbol{\sigma}_{13}^1 = 0$. Therefore, the inequality (D8) becomes:

$$|\boldsymbol{\sigma}_{11}^i| \leqslant \bar{\boldsymbol{\sigma}}_t^i$$

Thus, the maximal value of $\Sigma 1$, namely the macroscopic tension failure is the mean value of tensions failure of each constituent. In addition, we see that this value coincides with the upper bound $B_M$.

*Tension path along* $y_2$ *axis*. The multilayered material is subjected to simple tension in direction perpendicular to stratification. The macroscopic stress tensor is defined from the microscopic one using eqns (D4)–(D7) and the following relations.

$$\boldsymbol{\Sigma}_{11} = w_1\boldsymbol{\sigma}_{11}^1 + w_2\boldsymbol{\sigma}_{11}^2 = 0 \tag{D9}$$

$$\boldsymbol{\Sigma}1 = \boldsymbol{\sigma}_{22}^1 = \boldsymbol{\sigma}_{22}^2. \tag{D10}$$

The symmetry of this problem in relation to $y_2$-axis implies the following conditions:

$$\boldsymbol{\sigma}_{11}^\alpha = \boldsymbol{\sigma}_{33}^\alpha. \tag{D11}$$

In taking account of (D5), (D7), (D10) and (D11), we see that the Von Mises yield criterion is expressed in the $\alpha$th constituent as follows:

$$(\boldsymbol{\Sigma}1 - \boldsymbol{\sigma}_{11}^\alpha)^2 + 3(\boldsymbol{\sigma}_{13}^\alpha)^2 \leqslant (\bar{\boldsymbol{\sigma}}_t^\alpha)^2.$$

This inequality can be rewritten in the form:

$$-\sqrt{C_\sigma^\alpha} \leqslant (\boldsymbol{\Sigma}1 - \boldsymbol{\sigma}_{11}^\alpha) \leqslant \sqrt{C_\sigma^\alpha}$$

where

$$C_\sigma^\alpha \text{ denotes } (\bar{\boldsymbol{\sigma}}_t^\alpha)^2 - 3(\boldsymbol{\sigma}_{13}^\alpha)^2.$$

We multiply each part of the previous inequalities by the volume fraction of $\alpha$th constituent and we sum them. By taking into account of formula (D9), we obtain an upper bound of $\boldsymbol{\Sigma}1$:

$$\boldsymbol{\Sigma}1 \leqslant C_M \text{with } C_M = w_1\sqrt{C_\sigma^1} + w_2\sqrt{C_\sigma^2}.$$

By considering relation (D6), this upper bound can be rewritten as follows:

$$C_M = w_1\sqrt{(\bar{\boldsymbol{\sigma}}_t^1)^2 - 3(\boldsymbol{\sigma}_{13}^1)^2} + w_2\sqrt{(\bar{\boldsymbol{\sigma}}_t^2)^2 - 3\left(\frac{w_1}{w_2}\boldsymbol{\sigma}_{13}^1\right)^2}.$$

We can seek a maximal value of this upper bound by calculating the partial derivative of $C_M$ with respect to $\boldsymbol{\sigma}_{13}^1$.

$$\frac{\partial C_M}{\partial \boldsymbol{\sigma}_{13}^1} = -6w_1\boldsymbol{\sigma}_{13}^1\left(\frac{1}{\sqrt{C_\sigma^1}} + \frac{w_1}{w_2\sqrt{C_\sigma^2}}\right).$$

Thus, the maximal value of the upper bound $C_M$ is $w_1\bar{\boldsymbol{\sigma}}_t^1 + w_2\bar{\boldsymbol{\sigma}}_t^2$ (obtained when $\boldsymbol{\sigma}_{13}^1 = 0$). In other words, the simple tension failure of the homogenized material in direction perpendicular to stratification is the mean value of simple tensions failure of each constituent.